ChemPubSoc Europe

DOI: 10.1002/open.201900273

Open Access ChemistryOPEN Full Papers

Hyperpolarization of Pyridyl Fentalogues by Signal Amplification By Reversible Exchange (SABRE)

Thomas B. R. Robertson,[a] Lysbeth H. Antonides,[a, d] Nicolas Gilbert,[a, b] Sophie L. Benjamin,[c] Stuart K. Langley,[a] Lindsey J. Munro,[a] Oliver B. Sutcliffe,*[a, b] and Ryan E. Mewis*[a]

Fentanyl, also known as 'jackpot', is a synthetic opiate that is 50–100 times more potent than morphine. Clandestine laboratories produce analogues of fentanyl, known as fentalogues to circumvent legislation regarding its production. Three pyridyl fentalogues were synthesized and then hyperpolarized by signal amplification by reversible exchange (SABRE) to appraise the forensic potential of the technique. A maximum enhancement of -168-fold at 1.4 T was recorded for the *ortho* pyridyl ^{1}H nuclei. Studies of the activation parameters for the three fentalogues revealed that the ratio of ligand loss *trans* to hydride and hydride loss in the complex $[Ir(IMes)(L)_3(H)_2]^+$ (IMes = 1,3-*bis*(2,4,6-trimethylphenyl)imidazole-2-ylidene) ranged from 0.52 to 1.83. The fentalogue possessing the ratio closest to unity produced the largest enhancement subsequent to performing SABRE at earth's magnetic field. It was possible to hyperpolarize a pyridyl fentalogue selectively from a matrix that consisted largely of heroin (97:3 heroin:fentalogue) to validate the use of SABRE as a forensic tool.

1. Introduction

Hyperpolarization techniques are regularly employed to overcome the inherent sensitivity issue that is associated with NMR, and by extension, MRI. The inherent insensitivity arises due to the small population differences of the energy states that it probes. Dynamic nuclear polarization (DNP),[1] quantum-rotor induced polarisation,[2] spin-exchange optical pumping (SEOP)[1c,3] and *para*hydrogen induced polarization (PHIP)[1b,c] are four hyperpolarization methods that lead to improved population differences. Thus, these methods are extensively used for the analysis and detection of metabolites or pharmaceuticals,[4] catalytic intermediates[5] and for medical imaging purposes.[6]

PHIP utilises *para*hydrogen, a nuclear singlet, as the source of polarization. Polarization is transferred to a molecule of interest through a hydrogenative process resulting in chemical change. The result of polarization transfer creates a non-Boltzmann distribution of nuclear spins in the analyte thus meaning that the signals are noticeably enhanced in the ^{1}H NMR spectrum, for example. Precursors possessing the correct functionality, therefore, need to be prepared in order for the polarized molecule to be produced. A now established non-hydrogenative *para*hydrogen-based technique is Signal Amplification By Reversible Exchange (SABRE).[7] As this technique is non-hydrogenative, the analyte molecule is chemically unchanged during the polarization process. An iridium centred catalyst is typically employed to propagate polarisation, *via* J-coupling, between the *para*hydrogen derived hydrides and the spin-$^1/_2$ nuclei of the analyte molecule being polarised.[8] The pre-catalyst, [Ir(IMes)(COD)Cl] (IMes = 1,3-*bis*(2,4,6-trimethylphenyl)imidazole-2-ylidene, COD = cyclooctadiene) has been shown to be an excellent catalyst, following activation, in this regard for a number of substrates such as nicotinamide,[9] quinazoline,[10] and niacin.[11] Manipulation of the spin-reservoir of the substrate, such as deuteration, has been shown to be an effective route by which polarization can be maximized. This has been exemplified for methyl-4,6-d_2-nicotinate which was polarized to a level of 50%.[12]

Fentanyl (**1**, Figure 1), is regarded as a synthetic opiate, despite the chemical structure differing significantly from morphine, codeine and heroin (**2a**–**2c**), which are natural opiates. **1** exhibits a strong affinity towards the μ-opioid receptor, which is found across the central and peripheral nervous system as well as the intestinal tract and thus acts in a similar way to **2a**–**2c**. Activation of the μ-opioid receptor leads to analgesia and euphoria, but also physical dependence, constipation and respiratory depression,[13] which can lead to death in the case of an overdose.

[a] T. B. R. Robertson, L. H. Antonides, N. Gilbert, Dr. S. K. Langley, Dr. L. J. Munro, Dr. O. B. Sutcliffe, Dr. R. E. Mewis
Department of Natural Sciences
Manchester Metropolitan University
John Dalton Building, Chester St., Manchester, M1 5GD, UK
E-mail: r.mewis@mmu.ac.uk
o.sutcliffe@mmu.ac.uk
[b] N. Gilbert, Dr. O. B. Sutcliffe
MANchester DRug Analysis and Knowledge Exchange (MANDRAKE)
Manchester Metropolitan University
John Dalton Building, Chester St., Manchester, M1 5GD, UK
E-mail: o.sutcliffe@mmu.ac.uk
[c] Dr. S. L. Benjamin
School of Science and Technology
Nottingham Trent University
Nottingham, NG11 8NS, UK
[d] L. H. Antonides
Leverhulme Research Centre for Forensic Science
University of Dundee
Dundee, DD1 5EH, UK

Supporting information for this article is available on the WWW under https://doi.org/10.1002/open.201900273

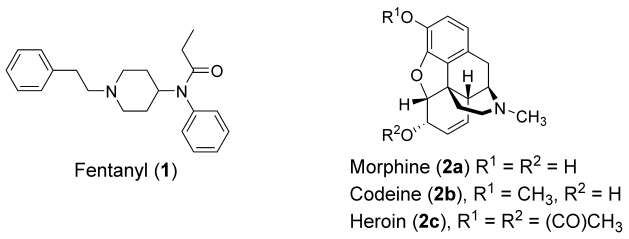

Figure 1. Chemical structures of common opiates.

1 attained widespread medical use due to its very strong and fast action, estimated at around 50–100 times stronger than **2a**.[14] Because of its euphoria-inducing effects, resembling those of **2c**, fentanyl has been used recreationally and is often referred to as 'jackpot'. This poses a serious threat for public health, as minute quantities of **1** (around 2 mg) can be enough to induce overdose.[15] This problem has been exacerbated as some heroin samples are contaminated with **1**, unbeknown to the end user[16] and as such, techniques have been developed for its detection.[17] Illicit sources of **1** are obtained by diversion of pharmaceutical supplies and *via* clandestine production.[18] The first large outbreak of deaths happened in California between 1979 and 1988, where 112 deaths were related to α-methylfentanyl abuse, and frequent incidents have been reported since then. From 2013 onward, however, abuse of **1** has grown significantly in the US, eventually reaching epidemic levels.[19] Recently, in 2016, 63,632 people died in the USA from a drug overdose, which is a 21% increase from the previous year.[20] This was largely attributed to a rise in deaths associated with pharmaceutical opioids, including **1** and its derivatives. In Europe, the problem has remained entrenched in Estonia, but cases have been observed in other countries,[18] including the UK.[16,21] Indeed, a worrying trend is the appearance of new fentanyl analogues, termed fentalogues, of which some are even more potent than **1**, on the international drug market scene. Since 2009, 18 new fentalogues have been detected by the European Monitoring Centre for Drugs and Drug Addiction (EMCDDA), and that number keeps growing every year.[22]

A number of techniques have been employed for the detection of fentanyl. Raman spectroscopy has been utilized in combination with density-functional theory (DFT) towards detection of trace samples. Surface-enhanced Raman spectroscopy proved to give an enhancement factor of $\geq 1.6\times10^5$, which was endowed by proximity to silver or gold nanoparticles.[23] Immunoassay has also been investigated as a technique for the detection of fentalogues, but none of the ELISA (Enzyme-Linked Immunosorbent Assay) kits evaluated proved to have sufficient cross-reactivity towards the *N*-acyl and piperidine-modified fentalogues studied.[24] LC-MS/MS (Liquid Chromatography-Mass Spectrometry/ Mass Spectrometry) has been utilized to detect 24 fentanyl derivatives and metabolites in whole blood in under 14 min screening time.[25] In addition, a dual HPLC-DAD (High-Performance Liquid Chromatography Diode-Array Detector) and HPLC-AD (Amperometric Detection) protocol that uses screen-printed graphite macroelectrodes for amperometric detection has been developed for the simultaneous detection of **1**, **2c** and ten fentalogues.[26] Furthermore, low-field (62 MHz) NMR spectroscopy has been used to differentiate 65 fentalogues in conjunction with quantum mechanical spin system analysis of spectra acquired at a frequency of 600 MHz to produce comparison spectra.[27] Low-field NMR was selected in this instance due to the cost saving attributes it possesses (smaller footprint, no need for cryogens, cheaper instrument cost) over high field instrumentation.

Given the low-threshold for overdose, we sought to employ an NMR-based methodology for detecting fentanyl or its pyridyl-analogues (**5**, **7** and **10**), which are synthesized as part of this work. Furthermore, we sought to demonstrate that a fentalogue can be readily detected despite being in a matrix consisting of largely of **2c** (97% w/w). In order to detect the fentalogue present in a single scan, thus avoiding the need for extensive instrument time, whilst also overcoming the inherent insensitivity associated with NMR, SABRE was employed to significantly enhance the signal intensity observed for the analogue of interest.

2. Results and Discussion

As a number of fentalogues have been encountered, three pyridyl-fentanyl analogues were also prepared to study alongside **1** and its hydrochloride salt. Fentalogues can be easily prepared through the replacement of the ethyl chain by selecting the desired acyl chloride instead of propanoyl chloride. Pyridine was one of the first compounds to be polarized by SABRE,[7,28] due to the initial use of Crabtree's catalyst, $[Ir(Py)(COD)PCy_3]^+$ (Py = pyridine, PCy_3 = tricyclohexylphosphine), or its derivatives, as a polarization transfer catalyst. Pyridine has been the focus of numerous studies,[29] and therefore, the pyridyl derivative was produced (**5**). Given the structural similarity of benzene and pyridine, two further analogues of **1** were synthesized which exchanged one of the benzene rings for pyridine (**7** and **10**). The addition of pyridyl rings to a peptide chain resulted in successful polarization by SABRE.[30] A similar approach has been used for the production of hyperpolarizable NOS (nitric oxide synthase) substrates.[31]

An overview of the synthesis of fentanyl derivatives is shown in Scheme 1. The synthesis of **1**.HCl and **5** utilized a two-step synthesis from 1-phenylethyl-4-piperidone (**3**) *via* the intermediate *N*-[1-(2-phenylethyl)-4-piperidinyl]aniline (**4**, 4-ANPP) which was synthesized according to a procedure reported by Valdez *et al.*[14] Yields for converting **4** to **1**.HCl and **5** were 33 and 45% respectively.

Fentalogue **7**, where the aniline group is substituted with a *N*-4-pyridine moiety, was prepared from **3** via reductive amination using 4-aminopyridine and $NaBH_4$ to afford the product (**6**) after purification in 22% yield. This compound was then converted to **7** by reacting it with propionic anhydride and isolated in 75% yield. The 2-furyl and 3-furyl derivatives of **7** have been produced by Bagley *et al.* in yields of 74% and 43% respectively,[32] in addition to substituting the chiral

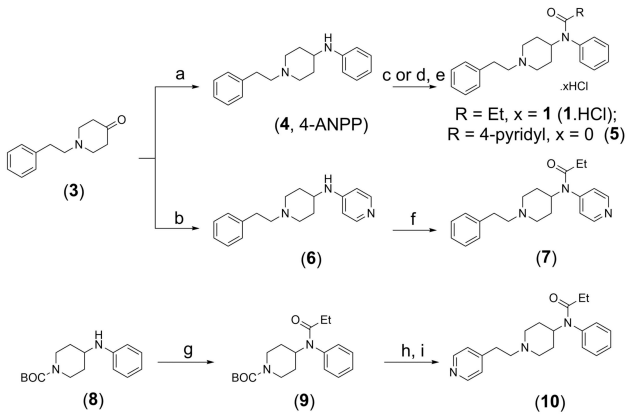

Scheme 1. Synthesis of fentanyl (**1**) and its pyridyl derivatives (**5**, **7** and **10**). Conditions: (a) $PhNH_2$, $NaBH(OAc)_3$; (b) 4-aminopyridine, $NaBH_4$; (c) EtCOCl, NEt_3; (d) 4-pyridinecarbonylchloride, NEt_3; (e) for **1**.HCl only: HCl (3 M in CPME); (f) $(EtCO)_2O$, toluene; (g) EtCOCl / $^iPr_2NEt$, DCM; (h) TFA-DCM (2:1); (i) 4-vinylpyridine, $MeO(CH_2)_2OH$

hydrogen of the piperidine ring with CO_2CH_3 and CH_2OCH_3 groups to study the pharmacological activity of the derivatives synthesized.[33]

Pyridylfentanyl, **10**, was synthesized by simple replacement of the phenethyl side-chain of **1** with a 4-pyridylethyl moiety. We hypothesized that inserting the pyridine ring further away from the bulk of the molecule, when compared with **5** and **7**, would result in a more efficient ligation (due to reducing steric interactions at the binding site) onto the iridium catalyst used in SABRE, leading to a greater signal enhancement. **10** was thus prepared in two steps from the BOC-protected precursor, **8**, in 59% yield. To ensure authenticity of the materials utilized in this study the synthesized materials were structurally characterized (see Supplementary Information) by NMR, FTIR and GC-EI-MS.

Slow evaporation of an acetone solution of **1**.HCl led to crystals suitable for X-ray crystallographic analysis. The salt crystalizes in the monoclinic space group *Cc*; the Ortep diagram of **1**.HCl is shown in Figure 2. The asymmetric unit contains the entire compound and a chloride counterion. The molecule crystallises in an extended and relatively planar conformation with only the *N*-phenyl ring deviating.

The piperidine ring present is in the chair conformation. Conformational pathway analysis of the chair and boat forms of piperidine have shown that the chair is the more stable conformer, similar to cyclohexane.[34] On inspection of the piperidine ring of **1**.HCl, it was found to have $^4C_1$ conformation and possessed the ring puckering parameters[35] $Q = 0.589$ Å, $q_2 = 0.025$ Å, $q_3 = 0.589$, $\Phi_2 = -27°$ and $\theta = 2.4°$ which were calculated using triangular decomposition.[36] As $q_3 \gg q_2$, the ring is a slightly distorted chair; the same observation was made for the free-base[37] and the citrate toluene solvate[38] of **1**.

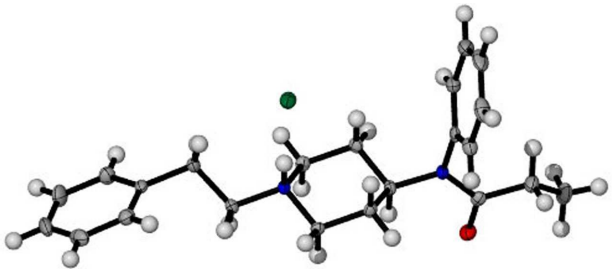

Figure 2. Ortep diagram of **1**.HCl with all atoms shown. The thermal ellipsoids for all non-H atoms are shown at the 50% level.

A search of the Cambridge Structural Database (CSD)[39] identified 26 other compounds with structural similarity to **1**.HCl. This search revealed that three further fentanyl derivatives have been crystallised that differ only in the length of a carboxylic acid chain present.[40] In all of the X-ray structures of these compounds, the piperidine ring is always in the chair conformation. In addition, the packing of molecules in the unit lattice shows a similar extended planar conformation as observed for **1**.HCl.

A hydrogen bond is present in **1**.HCl between N2-H2 and Cl1 and has a length of 2.12 Å. This value, along with the value of $D\cdots X^-$ (3.046 Å), compare well with reported mean values for this interaction.[41] Further parameters that detail this bond are shown in Table 1.

In this study, [Ir(IMes)(COD)Cl] was utilized as the SABRE pre-catalyst. Upon exposure to an excess of **5**, the complex $[Ir(IMes)(\mathbf{5})_3(H)_2]^+$ was formed; this complex is responsible for polarization transfer by SABRE, which is detailed later. The ^1H NMR spectrum of this complex possesses a main hydride signal at −23.17 ppm, which is indicative of chemically equivalent hydride ligands. Two smaller hydrides are also seen at −23.52 and −25.56 ppm; these are due to inequivalent hydrides in $[Ir(IMes)(\mathbf{5})_2(MeOH)(H)_2]^+$. Relative integrals of the hydride signals present indicate that the hydride signal for $[Ir(IMes)(\mathbf{5})_3(H)_2]^+$ dominates as they are present in a ratio of 98:2 compared to the hydride signals for $[Ir(IMes)(\mathbf{5})_2(MeOH)(H)_2]^+$. A similar observation has been made when pyridine is the analyte in that $[Ir(IMes)(Py)_2(MeOH)(H)_2]^+$ was detected.[29f] Due to the relative size of the signals for $[Ir(IMes)(\mathbf{5})_2(MeOH)(H)_2]^+$ compared to $[Ir(IMes)(\mathbf{5})_3(H)_2]^+$, characterization of the former complex was impractical. Of the three fentanyl ligands in $[Ir(IMes)(\mathbf{5})_3(H)_2]^+$, two are *trans* to hydride whereas the remaining ligand is *trans* to IMes. Due to the overlapping nature of the backbone of **5** for the free and the two bound forms, NMR-based studies focused largely on the pyridyl resonances which were sufficiently resolved for structural characterization of the complexes. The *ortho* proton signal of the pyridine ring of **5** *trans* to hydride is observed at δ 7.69 whereas the *meta* proton signal is at δ 6.75. The same signals for **5** *trans* to IMes are observed at δ 7.25 and 6.53 respectively. Using exchange spectroscopy (EXSY), the loss of hydride from $[Ir(IMes)(\mathbf{5})_3(H)_2]^+$ proved to be 5.6 s^{-1} at 300 K. This contrasts to 9 s^{-1} when $[Ir(IMes)(Py)_3(H)_2]^+$ was probed under the same conditions.[29e] The loss of hydride is, therefore,

Table 1. Hydrogen-bond geometry (Å, °) for **1**.HCl.

D–H···X–	D–H	H·· X–	D·· X–	D–H·· X–
N2–H2···Cl1	0.93	2.12	3.046 (2)	171

Table 2. Thermodynamic activation parameters and exchange rates of the complexes $[Ir(IMes)(L)_3(H)_2]^+$ where L = **5**, **7**, **10** or Py.

		5	7	10	Py[a]
Hydride loss	ΔG_{300}/kJ mol^{-1}	67.6 ± 0.07	69.4 ± 0.16	66.9 ± 0.06	66.4 ± 0.3
	ΔH/kJ mol^{-1}	75.8 ± 1.4	75.7 ± 4.8	85.1 ± 1.5	79 ± 1
	ΔS/J mol^{-1} K^{-1}	27.4 ± 5.0	21.0 ± 16.4	60.5 ± 5.0	41 ± 3
Loss of ligand *trans* to hydride	ΔG_{300}/kJ mol^{-1}	67.4 ± 0.07	67.4 ± 0.05	68.4 ± 0.11	64 ± 2
	ΔH/kJ mol^{-1}	69.6 ± 1.2	69.7 ± 0.6	79.4 ± 2.4	93 ± 3
	ΔS/J mol^{-1} K^{-1}	7.44 ± 4.3	7.73 ± 2.2	36.6 ± 8.2	97 ± 9
Loss of hydride at 300 K/s^{-1}		5.6	3.0	6.8	9
Loss of ligand at 300 K/s^{-1}		5.4	5.5	3.5	11.7

[a] Data taken from reference 29e.

significantly slower in $[Ir(IMes)(\mathbf{5})_3(H)_2]^+$ compared to $[Ir(IMes)(Py)_3(H)_2]^+$. An Eyring-Polanyi plot of hydride loss produced values for ΔG (300 K), ΔH and ΔS of 67.6 ± 0.07 kJ mol^{-1}, 75.8 ± 1.4 kJ mol^{-1} and 27.4 ± 5.0 J mol^{-1} K^{-1} respectively. The value of ΔH suggests that the Ir–H bond is relatively strong and contrasts well to the same bond in $[Ir(IMes)(Py)_3(H)_2]^+$ (79 ± 1 kJ mol^{-1}).

The loss of **5** from $[Ir(IMes)(\mathbf{5})_3(H)_2]^+$ was also studied using EXSY. For this process, the rate of loss of **5** was found to be 5.4 s^{-1} at 300 K. Similar to the hydride loss rate, this process was again much slower than pyridine in the analogous complex $[Ir(IMes)(Py)_3(H)_2]^+$ (11.7 s^{-1}). ΔG (300 K), ΔH and ΔS proved to be 67.4 ± 0.07 kJ mol^{-1}, 69.6 ± 1.2 kJ mol^{-1} and 7.44 ± 4.3 J mol^{-1} K^{-1} respectively for this process. Compared with $[Ir(IMes)(Py)_3(H)_2]^+$, the Ir–N bond in $[Ir(IMes)(\mathbf{5})_3(H)_2]^+$ is much weaker and also there is far less entropic gain from reaching the transition state.

7 and **10** were treated similarly to **5**. The complexes formed were analogous to those formed for **5**. Hydride resonances were observed at −22.70 and −22.83 ppm for $[Ir(IMes)(\mathbf{7})_3(H)_2]^+$ and $[Ir(IMes)(\mathbf{10})_3(H)_2]^+$ respectively. Only a single hydride was observed in both cases. The hydride and loss of fentanyl ligand *trans* to hydride from the two complexes are shown in table 2. Derivatives **5** and **7** result in very similar exchange rates for the loss of ligand, whilst hydride loss is quicker for **5** than **7** at 300 K. The thermodynamic activation parameters for both **5** and **7** show significant similarity, despite the pyridine ring involved in binding being bound through either the amide nitrogen or the CO of the same amide.

When **10** is considered, relative to **5** and **7**, we note that the loss of **10** *trans* to hydride from $[Ir(IMes)(\mathbf{10})_3(H)_2]^+$ requires a considerable amount of energy, as reflected in the ΔH value (79.4 ± 2.4 kJ mol^{-1}). The value of ΔH is ~10 kJ mol^{-1} higher than the respective values for **5** and **7**, implying that the Ir–N bond in $[Ir(IMes)(\mathbf{10})_3(H)_2]^+$ is the strongest of the fentalogues investigated. In addition, loss of **10** results in the biggest gain in entropy of all the fentalogues studied. This suggests that $[Ir(IMes)(\mathbf{10})_3(H)_2]^+$ is the most energetically stable of the complexes investigated. Furthermore, the loss of hydride at 300 K from $[Ir(IMes)(\mathbf{10})_3(H)_2]^+$ is the quickest of all the fentalogues investigated herein. It is noteworthy that the loss of **10** from $[Ir(IMes)(\mathbf{10})_3(H)_2]^+$ occurs much slower than hydride loss, which, although unusual, has been reported for $[Ir(SiPr)(Py)_3(H)_2]^+$.[29f] Extension of this comparison to also consider the same values for the rate of loss of either hydride or pyridine from $[Ir(IMes)(Py)_3(H)_2]^+$ revealed that loss of hydride from $[Ir(IMes)(\mathbf{10})_3(H)_2]^+$ most closely resembled that of the former, whilst the loss of either **5** or **7** from $[Ir(IMes)(L)_3(H)_2]^+$ are similar to the value for the latter. As part of our study, we wanted to probe the effect of these exchange parameters on the extent of polarization transfer *via* SABRE by obtaining ^{1}H NMR hyperpolarized spectra.

Table 3. ^{1}H NMR signal enhancements for the *ortho* pyridyl protons of **5**, **7** or **10** (L) hyperpolarised using [Ir(IMes)(COD)Cl] (ratio of L:Ir(IMes)(COD)Cl] is 4:1)

	Enhancement value obtained after transfer of polarization in the field indicated	
Fentanyl derivative (L)	Earth's magnetic field	6.5 mT
5	−168	−79
7	−38	−2
10	−50	−14

Initial hyperpolarization studies were directed towards the hyperpolarization of **1** and **1**.HCl by SABRE. However, the lack of suitable ligation groups/atoms to the SABRE catalyst meant that conventional SABRE could not be employed, although it was attempted to validate the change in approach (no enhancement observed). Instead a combined SABRE-Relay[11] CASH (catalyst separated hyperpolarization)-SABRE[42] approach was utilized (see SI for details). However, this approach failed to yield any detectable signal enhancement for either analyte following polarization transfer in earth's magnetic field and subsequent detection in a 1.4 T field. This was again, perhaps, expected, given that polarization of amines by SABRE-Relay has only been exemplified for primary and secondary amines.[11,43] To the best of our knowledge, polarization of tertiary amines has not been reported. Focus therefore moved to the fentanyl derivatives bearing pyridyl motifs (**5**, **7** and **10**).

The incorporation of pyridyl rings in to the fentanyl structure means that they are candidates for conventional SABRE. To facilitate polarization transfer from *para*hydrogen derived hydrides to the pyridyl fentanyl derivatives, the pre-catalyst [Ir(IMes)(COD)Cl] was employed. Studies were conducted using one equivalent of [Ir(IMes)(COD)Cl] to four equivalents of fentanyl derivative (**5**, **7** and **10**) in their free-base forms.

5 was successfully polarized by SABRE following polarization transfer at earth's magnetic field (Figure 3). The *ortho*- and *meta*-^{1}H NMR signal of the pyridyl ring are observed as emission and absorption signals respectively (indicated as α and β

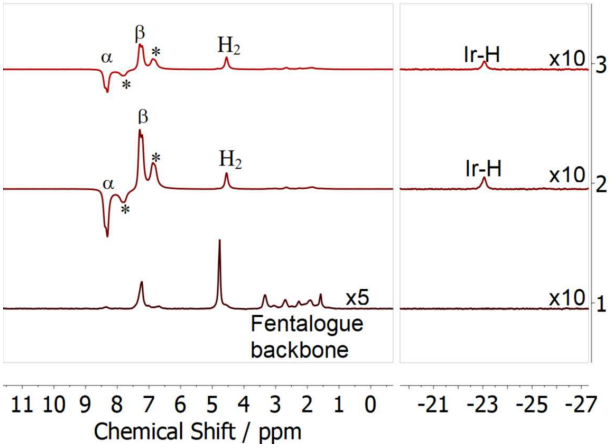

Figure 3. ^{1}H NMR spectra of **5** and [Ir(IMes)(COD)Cl] in the ratio of 4:1 in the presence of *para*hydrogen in CD_3OD. Spectrum 1 is the thermal spectrum whereas spectra 2 and 3 are hyperpolarized following polarization transfer in earth's magnetic field or at 6.5 mT respectively. Multiplication factors indicate scaling of the vertical axis. Spectra collected at 60 MHz. α and β refer to the *ortho*- and *meta*-pyridyl protons respectively of **5**. * indicates bound **5** of $[Ir(IMes)(\mathbf{5})_3(H)_2]^+$.

respectively in Figure 3). The *ortho* ^{1}H NMR signal (α) is enhanced by −168-fold. Due to the overlap of the phenyl ring protons with the *meta*-pyridyl protons (β), an enhancement for the latter cannot be calculated accurately. When the polarization transfer field was changed to 6.5 mT, the enhancement of the *ortho*-pyridyl protons fell to only −79-fold. A similar observation was made for NOS substrates bearing 4-substituted pyridyl-tethers.[31] The continuous re-hyperpolarization of nuclear spins has been explored theoretically, which has been shown to be dependent on the lifetime of the complex, as well as the magnetic field in which polarization is conducted.[44] The role of level-anti-crossings in the transfer of polarization has also been explored, and has been shown to be the most efficient at low magnetic fields.[45] Recently, a more simplified approach has been investigated, that takes in to account non-linear and chemical and physical dynamics to produce a master equation to provide insight in to the SABRE mechanism.[46]

No transfer is observed in to the piperidine ring of **5**. This was expected due to the vanishingly small size of the J_{HH}-couplings between the *meta*-pyridyl ring protons and the nearest piperidine ring protons.

We note here that the experiment is far from optimized. Critically, only 50% *para*hydrogen is employed. By utilizing 100% *para*hydrogen a further factor of three could be obtained for the enhancement values, as described by Shchepin and co-workers.[47] Furthermore, the magnetic field for polarization transfer was not optimized; only earth's field and a magnetic field of 6.5 mT were arbitrarily chosen for polarization transfer. As polarization occurs optimally when a level anti-crossing (LAC) condition is met,[45a,48] optimizing this parameter would yield even better enhancement values due to more efficient spin mixing. However, our goal was to simply demonstrate that the pyridyl fentalogues could be hyperpolarized, via SABRE, to obtain hyperpolarized ^{1}H NMR spectra.

7 was also polarized by SABRE following polarization transfer at earth's magnetic field. The *ortho*- and *meta*-^{1}H NMR signal of the pyridyl ring are again observed as emission and absorption signals respectively. In comparison to **5**, the enhancement observed was far lower (40-fold for both ^{1}H NMR sites of the pyridyl ring). The reductive elimination of hydride in $[Ir(IMes)(\mathbf{7})_2(H)_2]^+$ may result in slower polarization reservoir replenishment, thus leading to a smaller observed enhancement.

Hyperpolarization of **10** by SABRE produced ^{1}H NMR spectra that mirrored that of **5** and **7**. The *ortho*-pyridyl protons of **10** were enhanced by 50-fold. Unlike, **5** and **7**, it is not just the pyridyl ring protons that were hyperpolarized. The ethylene chain that connects the pyridine ring to that of the piperidine ring also show a small enhancement (small emissive peak at 2.65 ppm, see SI). 4-picoline, an analyte that is structurally similar to that of the ethylpyridine moiety has been investigated using SABRE, but the focus was on ^{15}N rather than ^{1}H polarization; no comment was made about the transfer to the methyl protons.[49] Compared with the enhancement of the *ortho*- and *meta*-pyridyl protons, the enhancement of the ethylene protons is significantly lower.

Comparison of the enhancement data for the fentalogues **5**, **7** and **10** to the thermodynamic activation parameters reported in table 2, reveals a number of interesting observations. **5** has the highest enhancement and the ratio of ligand loss *trans* to hydride to rate of hydride loss from $[Ir(IMes)(\mathbf{5})_3(H)_2]^+$ is 0.96. The rates of ligand loss *trans* to hydride and hydride loss are the most commensurate of the three fentalogues investigated; the corresponding ratios for **7** and **10** are 1.83 and 0.52 respectively. This gives the order **10** < **5** < **7**. Similarly, if the fentalogues are ordered in terms of their enhancements at earth's magnetic field, then the order is **5** > **10** > **7**. Thus, for pyridyl fentalogues **5**, **7** and **10**, the more commensurate the loss of ligand *trans* to hydride to loss of hydride is, the higher the enhancement. A similar trend is observed when polarization transfer is conducted in a magnetic field of 6.5 mT, although the values here are more susceptible to error due to the significant changes in magnetic field during transfer to the magnet when contrasted to performing the same experiment but shaking the tube in earth's magnetic field. A ±20% variation in enhancement values has been reported for the same sample when analyzed by different experimenters.[9b]

T_1 data was also collected for **5**, **7** and **10** (table 4). These data show there is little difference in the T_1s of **5**, **7** and **10** at the concentration investigated in the presence of $[Ir(IMes)(L)_3(H)_2]^+$ when L:$[Ir(IMes)(L)_3(H)_2]^+$ is 1:1. It is particularly noteworthy that in terms of the timescale of the experiment, in that following polarization transfer in the stated field to the application of a RF pulse inside the magnet, a whole T_1 is likely to have transpired resulting in significant loss of enhancement. Thus, elongating the T_1 of these molecules would significantly boost signal intensity. We note that compared to pyridine, in the presence of $[Ir(IMes)(Py)_3(H)_2]^+$ these T_1 values are 9 seconds shorter, which corresponds to a reduction of 75% of the T_1. The quicker relaxation of **5**, **7** and **10** is expected due to their increased molecular size compared to pyridine. Thus, the

Table 4. T_1 values at 298 K for *ortho* and *meta* pyridyl ^{1}H nuclei of free **5**, **7** or **10** in the presence or absence of $[Ir(IMes)(L)_3(H)_2]^+$ in d_4-MeOH and under a H_2 atmosphere, vacuum or in air. The concentration of L in all samples was 0.02 M. [a]Peak forms part of multiplet along with all the phenyl proton nuclei. T_1 listed is the value for all these different environments.

	T_1 in the presence of $[Ir(IMes)(\mathbf{L})_3(H)_2]^+$ and H_2/ s		T_1 (air)/s		T_1 under vacuum/s	
Fentanyl derivative (L)	*Ortho* ^{1}H nuclei	*Meta* ^{1}H nuclei	*Ortho* ^{1}H nuclei	Fentanyl derivative (L)	*Ortho* ^{1}H nuclei	*Meta* ^{1}H nuclei
5	3.1	3.5	2.6	**5**	3.1	3.5
7	2.9	3.2[a]	2.0	**7**	2.9	3.2[a]
10	3.3	2.1	2.3	**10**	3.3	2.1

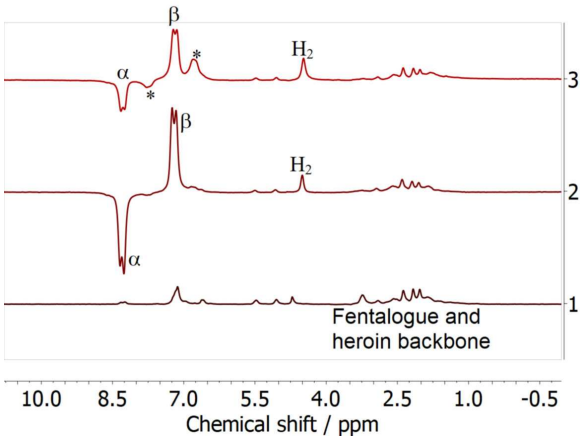

Figure 4. ^{1}H NMR spectra of **5** and heroin (3:97) [Ir(IMes)(COD)Cl] in the ratio of 4:1 in the presence of p-H_2 in CD_3OD. Spectrum 1 is the thermal spectrum whereas spectra 2 and 3 are hyperpolarized following polarization transfer in earth's magnetic field, with 3 being collected subsequent to 2. Spectra collected at 60 MHz. α and β refer to the *ortho*- and *meta*-pyridyl protons respectively of **5**. * indicates bound **5** of $[Ir(IMes)(\mathbf{5})_3(H)_2]^+$.

enhancements reported for **5**, **7** and **10** are significantly reduced by relaxation processes. To overcome these short T_1s, other nuclei such as ^{15}N, could be utilized, especially when combined with a heterogeneous approach.[50] Recent studies have shown that ^{15}N-based polarization can be detected at high-field via spin lock induced crossing (SLIC)-SABRE, which has been exemplified for pyridine and nicotinamide,[51] as well as dalfampridine, a drug which is used in the treatment of multiple sclerosis.[52] The pyridyl nitrogen of dalfampridine was enhanced by over 32,000-fold. Metronidazole, an antibiotic has been polarized to a level of 15%, which persists for tens of minutes at 1.4 T.[53] However, our focus here was to study the ^{1}H polarization, and lifetimes, only.

We also wanted to test the selectivity of the SABRE catalyst for the fentanyl derivatives described herein in the presence of heroin, given that they have similar pharmacological actions, yet fentanyl has a far lower LD_{50}, and hence is more potent, than heroin. Hyperpolarization of **2c** using [Ir(IMes)(COD)Cl] revealed no evidence for polarization transfer. This is despite **2a** having been polarized previously, albeit using the catalyst $[Ir(COD)(PCy_3)(py)][PF_6]$.[54] It is proposed that **2c** did not polarize under the conditions employed here are most likely due to heroin lacking a suitable donor to ligate to the catalyst in order to become hyperpolarized and / or steric hindrance preventing successful binding; no hydride signal was detected in the ^{1}H NMR spectra collected (see SI). **5** was selected as the fentalogue to test given the number of other derivatives that have been encountered that have been derivatized similarly by replacing the ethyl attached to the amide for other moieties, such as methoxyacetyl, isobutyl and isovaleryl, along with many others.[24–26] We have also evidenced that **5** shows the most significant enhancement by SABRE of the three fentalogues synthesized herein. A solution consisting of **5** and heroin (ratio 3:97 w/w) were subjected to SABRE. The amount of **5** present relative to [Ir(IMes)(COD)Cl] was 4:1. The resulting ^{1}H NMR spectrum (figure 4) provided evidence for **5** being polarized, namely the *ortho* ^{1}H NMR signal (indicated as α in figure 4) of free **5** at δ 8.25. Initially, the signal enhancement was 47-fold, but then fell to 24-fold in subsequent experiments. We note that this is a reduction of ~100-fold compared to the sample without heroin present, and this reduction represents the complexity of the matrix affecting effective ligation of **5** to the iridium species in solution. The *meta* pyridyl ^{1}H NMR resonance of free **5** also showed enhancement, but due to the overlapping nature of this ^{1}H NMR signal and the phenyl rings of **5** and those of heroin, an accurate enhancement could not be calculated.

3. Conclusions

This paper describes the successful synthesis of fentanyl derivatives that possess pyridine rings (**5**, **7** and **10**) that are polarized by SABRE. Enhancements of −168-fold, −38-fold and −50-fold are reported for the *ortho* pyridyl protons of **5**, **7** and **10** respectively despite the T_1s of these environments being in the region of 2.9–3.3 s, which are significantly shorter than pyridine. The thermodynamic activation parameters of ligand loss *trans* to hydride, where L = **5**, **7** or **10**, and hydride loss from $[Ir(IMes)(L)_3(H)_2]^+$ were obtained. The ratio of rate of ligand loss *trans* to hydride, to rate of hydride loss was calculated (**5** = 0.96, **7** = 1.83 and **10** = 0.52) and the order **10** < **5** < **7** was established. The trend observed for the enhancement observed at earth's magnetic field was **5** > **10** > **7**, thus highlighting that for **5**, **7** and **10**, the more commensurate the loss of ligand *trans* to hydride to loss of hydride is, the higher the enhancement.

SABRE was employed to hyperpolarize one of the fentanyl derivatives, **5**, which represents an easily accessible fentalogue, based on the synthesis described herein, that could be produced by a clandestine laboratory. A matrix that largely consisted of heroin (ratio 97:3 heroin:**5**) resulted in the *ortho* pyridyl protons of **5** being enhanced by 47-fold, which fell to 24-fold in subsequent polarization-based experiments. It was not possible to polarize heroin using the pre-catalyst [Ir(IMes)(COD)Cl] under the conditions employed herein. However, the selective hyperpolarization of **5** showcases the potential for SABRE as a forensic tool in order to validate the presence of

pyridyl fentalogues in a sample, should these be produced by clandestine laboratories.

Experimental Section

Full details of the synthesis and characterization of **1**–**10**, the methodology for conducting the hyperpolarisation-based experiments, calculation of ^{1}H NMR enhancement factors, exchange rate data and ring puckering parameter calculations can be found in the Supporting Information. CCDC1937850 contains the supplementary crystallographic data for this paper. These data are provided free of charge by The Cambridge Crystallographic Data Centre.

Acknowledgements

REM is grateful to Manchester Metropolitan University for a Vice Chancellor studentship for TBRR. The Natural Sciences and Engineering Research Council of Canada (396154510) and Fonds de Recherche du Québec - Nature et Technologie (206375) are thanked for funding for NG. Oxford Instruments, especially Hetal Patel, are thanked for their technical support.

Conflict of Interest

The authors declare no conflict of interest.

Keywords: NMR · fentanyl · fentalogues · hyperpolarisation · exchange dynamics

[1] a) G. N. Zhang, C. Hilty, *Magn. Reson. Chem.* **2018**, *56*, 566–582; b) K. V. Kovtunov, E. V. Pokochueva, O. G. Salnikov, S. F. Cousin, D. Kurzbach, B. Vuichoud, S. Jannin, E. Y. Chekmenev, B. M. Goodson, D. A. Barskiy, I. V. Koptyug, *Chem. Asian J.* **2018**, *13*, 1857–1871; c) C. Witte, L. Schroder, *NMR Biomed.* **2013**, *26*, 788–802.

[2] B. Meier, *Magn. Reson. Chem.* **2018**, *56*, 610–618.

[3] T. R. Gentile, P. J. Nacher, B. Saam, T. G. Walker, *Rev. Mod. Phys.* **2017**, *89*.

[4] a) L. Zhao, A. C. Pinon, L. Emsley, A. J. Rossini, *Magn. Reson. Chem.* **2018**, *56*, 583–609; b) C. H. Chen, Y. Y. Wang, C. Hilty, *Methods* **2018**, *138*, 69–75.

[5] a) S. B. Duckett, R. E. Mewis, *Acc. Chem. Res.* **2012**, *45*, 1247–1257; b) K. V. Kovtunov, V. V. Zhivonitko, I. V. Skovpin, D. A. Barskiy, I. V. Koptyug, *Hyperpolarization Methods in Nmr Spectroscopy, Vol. 338* (Ed.: L. T. Kuhn), **2013**, pp. 123–180; c) A. Viale, D. Santelia, R. Napolitano, R. Gobetto, W. Dastru, S. Aime, *Eur. J. Inorg. Chem.* **2008**, 4348–4351.

[6] a) A. Apps, J. Lau, M. Peterzan, S. Neubauer, D. Tyler, O. Rider, *Heart* **2018**, *104*, 1484; b) J. G. Skinner, L. Menichetti, A. Flori, A. Dost, A. B. Schmidt, M. Plaumann, F. A. Gallagher, J. B. Hovener, *Mol. Imaging Biol.* **2018**, *20*, 902–918; c) E. Cavallari, C. Carrera, S. Aime, F. Reineri, *ChemPhysChem* **2019**, *20*, 318–325; d) D. P. Downes, J. H. P. Collins, B. Lama, H. D. Zeng, T. Nguyen, G. Keller, M. Febo, J. R. Long, *ChemPhysChem* **2019**, *20*, 216–230; e) J. W. Gordon, H. Y. Chen, A. Autry, I. Park, M. Van Criekinge, D. Mammoli, E. Milshteyn, R. Bok, D. Xu, Y. Li, R. Aggarwal, S. Chang, J. B. Slater, M. Ferrone, S. Nelson, J. Kurhanewicz, P. E. Z. Larson, D. B. Vigneron, *Magn. Reson. Med.* **2019**, *81*, 2702–2709.

[7] R. W. Adams, J. A. Aguilar, K. D. Atkinson, M. J. Cowley, P. I. P. Elliott, S. B. Duckett, G. G. R. Green, I. G. Khazal, J. López-Serrano, D. C. Williamson, *Science* **2009**, *323*, 1708–1711.

[8] R. W. Adams, S. B. Duckett, R. A. Green, D. C. Williamson, G. G. R. Green, *J. Chem. Phys.* **2009**, *131*.

[9] a) J. B. Hovener, N. Schwaderlapp, R. Borowiak, T. Lickert, S. B. Duckett, R. E. Mewis, R. W. Adams, M. J. Burns, L. A. R. Highton, G. G. R. Green, A. Olaru, J. Hennig, D. von Elverfeldt, *Anal. Chem.* **2014**, *86*, 1767–1774; b) R. E. Mewis, K. D. Atkinson, M. J. Cowley, S. B. Duckett, G. G. R. Green, R. A. Green, L. A. R. Highton, D. Kilgour, L. S. Lloyd, J. A. B. Lohman, D. C. Williamson, *Magn. Reson. Chem.* **2014**, *52*, 358–369; c) T. Theis, M. L. Truong, A. M. Coffey, R. V. Shchepin, K. W. Waddell, F. Shi, B. M. Goodson, W. S. Warren, E. Y. Chekmenev, *J. Am. Chem. Soc.* **2015**, *137*, 1404–1407; d) M. L. Truong, F. Shi, P. He, B. X. Yuan, K. N. Plunkett, A. M. Coffey, R. V. Shchepin, D. A. Barskiy, K. V. Kovtunov, I. V. Koptyug, K. W. Waddell, B. M. Goodson, E. Y. Chekmenev, *J. Phys. Chem. B* **2014**, *118*, 13882–13889.

[10] J. E. Richards, A. J. J. Hooper, O. W. Bayfield, M. C. R. Cockett, G. J. Dear, A. J. Holmes, R. O. John, R. E. Mewis, N. Pridmore, A. D. Roberts, A. C. Whitwood, S. B. Duckett, *Chem. Commun.* **2018**, *54*, 10375–10378.

[11] S. S. Roy, K. M. Appleby, E. J. Fear, S. B. Duckett, *J. Phys. Chem. Lett.* **2018**, *9*, 1112–1117.

[12] P. J. Rayner, M. J. Burns, A. M. Olaru, P. Norcott, M. Fekete, G. G. R. Green, L. A. R. Highton, R. E. Mewis, S. B. Duckett, *PNAS* **2017**, *114*, E3188–E3194.

[13] V. Spahn, G. Del Vecchio, D. Labuz, A. Rodriguez-Gaztelumendi, N. Massaly, J. Temp, V. Durmaz, P. Sabri, M. Reidelbach, H. Machelska, M. Weber, C. Stein, *Science* **2017**, *355*, 966–969.

[14] C. A. Valdez, R. N. Leif, B. P. Mayer, *PLoS One* **2014**, *9*.

[15] R. S. Vardanyan, V. J. Hruby, *Future Med. Chem.* **2014**, *6*, 385–412.

[16] P. Bijral, K. P. Hayhurst, S. M. Bird, T. Millar, *Clin. Toxicol.* **2019**, *57*, 368–371.

[17] R. Salemmilani, M. Moskovits, C. D. Meinhart, *Analyst* **2019**, *144*, 3080–3087.

[18] J. Mounteney, I. Giraudon, G. Denissov, P. Griffiths, *Int. J. Drug Deliv.* **2015**, *26*, 626–631.

[19] P. Armenian, K. T. Vo, J. Barr-Walker, K. L. Lynch, *Neuropharmacology* **2018**, *134*, 121–132.

[20] P. Seth, L. Scholl, R. A. Rudd, S. Bacon, *MMWR* **2018**, *67*, 349–358.

[21] L. Hikin, P. R. Smith, E. Ringland, S. Hudson, S. R. Morley, *Forensic Sci. Int.* **2018**, *282*, 179–183.

[22] European Monitoring Centre for Drugs and Drug Addiction, **2017**.

[23] J. Leonard, A. Haddad, O. Green, R. L. Birke, T. Kubic, A. Kocak, J. R. Lombardi, *J. Raman Spectrosc.* **2017**, *48*, 1323–1329.

[24] M. Schackmuth, S. Kerrigan, *Forensic Toxicol.* **2019**, *37*, 231–237.

[25] K. E. Strayer, H. M. Antonides, M. P. Juhascik, R. Daniulaityte, I. E. Sizemore, *ACS Omega* **2018**, *3*, 514–523.

[26] H. M. Elbardisy, C. W. Foster, L. Cumba, L. H. Antonides, N. Gilbert, C. J. Schofield, T. S. Belal, W. Talaat, O. B. Sutcliffe, H. G. Daabees, C. E. Banks, *Anal. Methods* **2019**, *11*, 1053–1063.

[27] J. Duffy, A. Urbas, M. Niemitz, K. Lippa, I. Marginean, *Anal. Chim. Acta* **2019**, *1049*, 161–169.

[28] K. D. Atkinson, M. J. Cowley, S. B. Duckett, P. I. P. Elliott, G. G. R. Green, J. Lopez-Serrano, I. G. Khazal, A. C. Whitwood, *Inorg. Chem.* **2009**, *48*, 663–670.

[29] a) A. N. Pravdivtsev, I. V. Skovpin, A. I. Svyatova, N. V. Chukanov, L. M. Kovtunova, V. I. Bukhtiyarov, E. Y. Chekmenev, K. V. Kovtunov, I. V. Koptyug, J. B. Hovener, *J. Phys. Chem. A* **2018**, *122*, 9107–9114; b) P. J. Rayner, P. Norcott, K. M. Appleby, W. Iali, R. O. John, S. J. Hart, A. C. Whitwood, S. B. Duckett, *Nat. Commun.* **2018**, *9*; c) P. Stepanek, C. Sanchez-Perez, V. V. Telkki, V. V. Zhivonitko, A. M. Kantola, *J. Mag. Res.* **2019**, *300*, 8–17; d) C. M. Wong, M. Fekete, R. Nelson-Forde, M. R. D. Gatus, P. J. Rayner, A. C. Whitwood, S. B. Duckett, B. A. Messerle, *Cat. Sci. Technol.* **2018**, *8*, 4925–4933; e) M. J. Cowley, R. W. Adams, K. D. Atkinson, M. C. R. Cockett, S. B. Duckett, G. G. R. Green, J. A. B. Lohman, R. Kerssebaum, D. Kilgour, R. E. Mewis, *J. Am. Chem. Soc.* **2011**, *133*, 6134–6137; f) L. S. Lloyd, A. Asghar, M. J. Burns, A. Charlton, S. Coombes, M. J. Cowley, G. J. Dear, S. B. Duckett, G. R. Genov, G. G. R. Green, L. A. R. Highton, A. J. J. Hooper, M. Khan, I. G. Khazal, R. J. Lewis, R. E. Mewis, A. D. Roberts, A. J. Ruddlesden, *Cat. Sci. Technol.* **2014**, *4*, 3544–3554.

[30] T. Ratajczyk, T. Gutmann, P. Bernatowicz, G. Buntkowsky, J. Frydel, B. Fedorczyk, *Chem. Eur. J.* **2015**, *21*, 12616–12619.

[31] F. F. Diaz-Rullo, F. Zamberlan, R. E. Mewis, M. Fekete, L. Broche, L. A. Cheyne, S. Dall'Angelo, S. B. Duckett, D. Dawson, M. Zanda, *Bioorg. Med. Chem.* **2017**, *25*, 2730–2742.

[32] J. R. Bagley, R. L. Wynn, F. G. Rudo, B. M. Doorley, H. K. Spencer, T. Spaulding, *J. Med. Chem.* **1989**, *32*, 663–671.

[33] J. R. Bagley, S. A. Thomas, F. G. Rudo, H. K. Spencer, B. M. Doorley, M. H. Ossipov, T. P. Jerussi, M. J. Benvenga, T. Spaulding, *J. Med. Chem.* **1991**, *34*, 827–841.

[34] C. A. Stortz, *J. Phys. Org. Chem.* **2010**, *23*, 1173–1186.

[35] D. Cremer, J. A. Pople, *J. Am. Chem. Soc.* **1975**, *97*, 1354–1358.

[36] A. D. Hill, P. J. Reilly, *J. Chem. Inf. Model.* **2007**, *47*, 1031–1035.
[37] N. Ogawa, H. Nagase, T. Endo, T. Loftsson, H. Ueda, *X-Ray Struct. Anal. Online* **2009**, *25*, 83–84.
[38] O. M. Peeters, N. M. Blaton, C. J. Deranter, A. M. Vanherk, K. Goubitz, *J. Cryst. Mol. Struct.* **1979**, *9*, 153–161.
[39] C. R. Groom, I. J. Bruno, M. P. Lightfoot, S. C. Ward, *Acta Crystallogr. Sect. B* **2016**, *72*, 171–179.
[40] G. S. Nichol, V. K. Kumirov, R. Vardanyan, V. J. Hruby, *CrystEngComm* **2010**, *12*, 3651–3657.
[41] T. Steiner, *Acta Crystallogr. Sect. B* **1998**, *54*, 456–463.
[42] W. Iali, A. M. Olaru, G. G. R. Green, S. B. Duckett, *Chem. Eur. J.* **2017**, *23*, 10491–10495.
[43] a) W. Iali, P. J. Rayner, A. Alshehri, A. J. Holmes, A. J. Ruddlesden, S. B. Duckett, *Chem. Sci.* **2018**, *9*, 3677–3684; b) P. M. Richardson, R. O. John, A. J. Parrott, P. J. Rayner, W. Iali, A. Nordon, M. E. Halse, S. B. Duckett, *Phys. Chem. Chem. Phys.* **2018**, *20*, 26362–26371; c) P. J. Rayner, B. J. Tickner, W. Iali, M. Fekete, A. D. Robinson, S. B. Duckett, *Chem. Sci.* **2019**, *10*, 7709–7717.
[44] J. B. Hovener, S. Knecht, N. Schwaderlapp, J. Hennig, D. von Elverfeldt, *ChemPhysChem* **2014**, *15*, 2451–2457.
[45] a) K. L. Ivanov, A. N. Pravdivtsev, A. V. Yurkovskaya, H. M. Vieth, R. Kaptein, *Prog. Nucl. Magn. Reson. Spectrosc.* **2014**, *81*, 1–36; b) A. N. Pravdivtsev, K. L. Ivanov, A. V. Yurkovskaya, P. A. Petrov, H. H. Limbach, R. Kaptein, H. M. Vieth, *J. Mag. Res.* **2015**, *261*, 73–82.
[46] A. N. Pravdivtsev, J. B. Hovener, *Chem. Eur. J.* **2019**, *25*, 7659–7668.
[47] R. V. Shchepin, D. A. Barskiy, A. M. Coffey, T. Theis, F. Shi, W. S. Warren, B. M. Goodson, E. Y. Chekmenev, *ACS Sens.* **2016**, *1*, 640–644.
[48] a) A. N. Pravdivtsev, A. V. Yurkovskaya, N. N. Lukzen, K. L. Ivanov, H. M. Vieth, *J. Phys. Chem. Lett.* **2014**, *5*, 3421–3426; b) A. N. Pravdivtsev, A. V. Yurkovskaya, H. M. Vieth, K. L. Ivanov, *Phys. Chem. Chem. Phys.* **2014**, *16*, 24672–24675.
[49] R. V. Shchepin, M. L. Truong, T. Theis, A. M. Coffey, F. Shi, K. W. Waddell, W. S. Warren, B. M. Goodson, E. Y. Chekmenev, *J. Phys. Chem. Lett.* **2015**, *6*, 1961–1967.
[50] K. V. Kovtunov, L. M. Kovtunova, M. E. Gemeinhardt, A. V. Bukhtiyarov, J. Gesiorski, V. I. Bukhtiyarov, E. Y. Chekmenev, I. V. Koptyug, B. M. Goodson, *Angew. Chem. Int. Ed.* **2017**, *56*, 10433–10437; *Angew. Chem.* **2017**, *129*, 10569–10573.
[51] A. Svyatova, I. V. Skovpin, N. V. Chukanov, K. V. Kovtunov, E. Y. Chekmenev, A. N. Pravdivtsev, J.-B. Hövener, I. V. Koptyug, *Chem. Eur. J.* **2019**, *25*, 8465–8470.
[52] I. V. Skovpin, A. Svyatova, N. Chukanov, E. Y. Chekmenev, K. V. Kovtunov, I. V. Koptyug, *Chemistry-A European Journal, 0*.
[53] R. V. Shchepin, J. R. Birchall, N. V. Chukanov, K. V. Kovtunov, I. V. Koptyug, T. Theis, W. S. Warren, J. G. Gelovani, B. M. Goodson, S. Shokouhi, M. S. Rosen, Y. F. Yen, W. Pham, E. Y. Chekmenev, *Chem. Eur. J.* **2019**, *25*, 8829–8836.
[54] S. Gloggler, M. Emondts, J. Colell, R. Muller, B. Blumich, S. Appelt, *Analyst* **2011**, *136*, 1566–1568.

Manuscript received: September 9, 2019
Revised manuscript received: September 24, 2019